THE JOURNAL OF PHYSICAL CHEMISTRY B

Article

pubs.acs.org/JPCB

Colloidal Model of Lysozyme Aqueous Solutions: A Computer Simulation and Theoretical Study

Giuseppe Pellicane*

School of Chemistry and Physics, University of Kwazulu-Natal, Private Bag X01, Scottsville 3209, Pietermaritzburg, South Africa

ABSTRACT: Lysozyme interactions in an aqueous solution are modeled via the Derjaguin−Landau−Verwey−Overbeek (DLVO) theory. We calculate the structural functions at different pH values by means of Monte Carlo computer simulation and integral equation theories. The theoretical structure factor is then used to evaluate the scattered intensities, which are compared with the experimental small-angle neutron scattering data reported in *Philos. Mag.* **2011**, *91*, 2066. We find that the DLVO theory reproduces only qualitatively the tendency of protein interactions to become more short-range and attractive at low ionic strength; however, at sufficiently high ionic strength, the theory becomes quantitative. At the higher investigated pH values, DLVO theory predicts the formation of protein aggregates driven by the competition of short-range attraction and long-range repulsion.

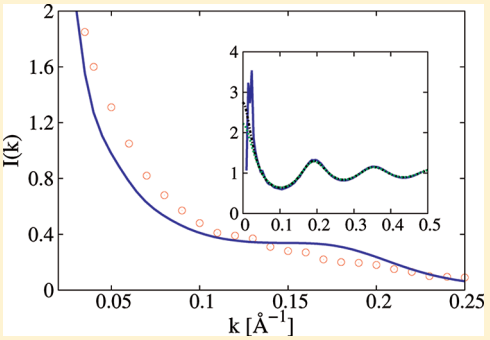

I. INTRODUCTION

Protein interactions in an aqueous solution are important in many biophysical and physiological processes. When a protein performs its biological function, the knowledge of the precise chemical nature and spatial location of its thousands of atoms becomes essential, especially when conformation changes occur. For example, huge protein complexes (e.g., ribosomal subunit assemblies[1,2]) are the result of a specific, molecular recognition process. Unfortunately, when we are interested in the collective behavior (e.g., protein crystallization[3] or demixing into two disordered protein phases[4]), we are forced to drop the atomistic description of protein solutions for computational reasons, and resort to coarse-grained models,[5] where the degrees of freedom of the solvent have been averaged out. In this framework, a globular protein is frequently depicted as a colloidal particle,[6] that is, a macromolecule with well-defined size and shape, instead of being considered as a long polymer (the polypeptide chain constituting the backbone of the protein) with multiple conformational degrees of freedom.

Colloidal interactions are by definition tunable ones,[7] and in the case of protein interactions, tunability can be exploited through the so-called salting-in effect, which is achieved by adding an electrolyte (salt plus acid buffer to stabilize the pH) to the solution.[8] Some of the ionizable groups on the protein surface dissociate in the presence of a polar liquid such as water. Whereas the ions of the electrolyte tend to form hydrogen bridges with the polar amino-acidic residues of the protein surface, the counterions discharged in the solvent move away from the protein surface but nevertheless remain in its field of force. This mechanism provides a coulomb-screened force between proteins, whose intensity can be tuned by modifying the electrolyte concentration, that is, the solution ionic strength. Another aspect supporting the application of colloidal models to globular proteins is the experimental evidence that protein crystals generally coexist with a dilute protein solution.[9] Then, the measured second virial coefficient B_2 (related to the osmotic equation of state) is observed to be slightly negative for these solution conditions.[10] Because the value of B_2 for a dilute solution can be straightforwardly related to the magnitude of protein interactions, this correlation has been frequently explained in terms of short-range attractive forces between proteins.[11−13] Short-range attraction is also observed in charge-screened colloidal particles, whose phase diagram shows only a fluid phase in thermodynamic equilibrium with a solid phase, with a metastable phase separation located underneath the crystallization curve.[13,14]

The colloidal point of view of protein interactions has been the object of intense debate[15−17] in the scientific community because its basic assumptions seem too oversimplifying for small macroparticles on the colloidal length scale, as proteins certainly are. For instance, the net charge on the protein surface is often limited to a few electron charges, whereas it amounts to thousands of charge units for real colloidal particles. This observation makes it difficult to accept the simple picture that the charge could be uniformly smeared-out on the protein surface because both the number of net charges and the length scale separating them are small compared with their counterparts in colloidal particles.[18] However, there is some evidence that suggests that further investigation of this issue could be well-deserved. In fact, colloidal models have been frequently adopted to estimate the nature of protein interactions in a number of experiments,[19−23] and they have also been successfully applied to predict the thermodynamic properties,[24] phase diagrams,[25,26] and structural functions.[22] Their success can be partially understood if we note that, for example, for lysozyme, the typical values of the translational D_T and of the

Received: December 14, 2011
Revised: January 22, 2012
Published: January 25, 2012

rotational D_R diffusion coefficients are $D_T \approx 10^{-6}$ cm^2 s^{-1} and $D_R \approx 10^7$ Hz;[27] that is, a protein rotates 10^7 times before it diffuses through the solution a distance on the order of its average linear length.

The goal of this Article is to gain a better insight into the merits of a colloidal representation of protein interactions. In this aim, we consider the paradigmatic Derjaguin–Landau–Verwey–Overbeek (DLVO[28,29]) model of colloidal interactions. We apply it to lysozyme, for which recent small-angle neutron scattering (SANS) intensity measurements are available in the literature,[30] and we perform *NVT* Monte Carlo (MC) computer simulations[31] to calculate the structural properties and, in particular, the scattered intensity. The comparison of the numerical intensity to the experimental data will allow us to assess the reliability of the DLVO theory as applied to lysozyme interactions under different solution conditions.

The novelty of this work is that we do not make recourse to any fitting parameters to reproduce the experimental structural quantities, which is a widely adopted procedure in the literature.[20,22,32] The only parameter that is adjusted to match the "magnitude" of the energy of interaction of solvated proteins is the Hamaker constant of the DLVO potential. Its value is independently estimated by setting the theoretical B_2 equal to the experimental B_2 value of the lysozyme solution at the critical temperature of the protein demixing region.[33] Therefore, within this approach, we let the functional form of the dispersion energy take into account other non-DLVO interactions (such as hydration or hydrophobic effects and hydrogen bonding). Accordingly, the Hamaker constant is inflated to values well beyond the dispersion contribution (which is on the order of the thermal energy k_BT). Because a number of different colloidal models have already been successfully applied to protein interactions (as, e.g., the hard-core Yukawa,[20] Baxter,[34] or modified Lennard-Jones potential[13]), we believe that the results should be independent of the exact shape of the attractive contribution to the potential energy, provided that such contribution is a short-range one. For instance, a generalized Lennard-Jones potential has been recently adopted to account properly for the attractive part,[35,36] and remarkable agreement was observed between experimental and numerical calculations for lysozyme solutions under no-added salt conditions. To the extent that we are not introducing any external bias to the electrostatic interaction of the DLVO model (i.e., we are not fitting any parameter to match the experimental scattered intensity), the comparison with the experimental structural data will allow us to spot the ionic strength regime of validity of the linearized Poisson–Boltzmann approximation, which underlies the DLVO theory.

By a different perspective, we will also compare the computer simulation results for the DLVO model with some predictions based on integral equation theories (IETs).[37,38] Because IETs are frequently adopted to calculate structural functions of colloidal models of protein solutions,[20,22,23] this analysis provides a useful insight *per se*.

The Article is organized as follows. In Section II, we describe the DLVO model and IETs and provide some technical details of the MC computer simulation. In Section III, we report the results and their discussion. Finally, in Section IV, we draw some conclusions.

II. MODEL AND NUMERICAL APPROACH

The DLVO model is a pair-interaction potential consisting of the sum of two energy contributions. The first one is the electrostatic potential originating in the Z_pe electronic charges on the protein surface. The repulsion between two proteins is screened by a layer of thermally agitated counterions, and provided this screening layer is sufficiently compact, it becomes reasonable to linearize the Poisson–Boltzmann equation to obtain

$$V_{DH}(r) = \frac{1}{4\pi\varepsilon_0\varepsilon_r}\left[\frac{Z_p e}{1 + \kappa_D\sigma_0/2}\right]^2 \frac{\exp[-\kappa_D(r - \sigma_0)]}{r} \tag{1}$$

where ε_0 is the vacuum permittivity, ε_r is the relative permittivity of the solvent, σ_0 is the average protein linear dimension (diameter), and κ_D is the Debye–Hückel inverse screening length given by

$$\kappa_D = \sqrt{\frac{2I_s e^2}{\varepsilon_0\varepsilon_r k_B T}} \tag{2}$$

Here I_s is the ionic strength of the solution, which accounts for the ion concentration due to the electrolytes added to the solution, k_B is the Boltzmann constant, and T is the absolute temperature.

The second contribution of the DLVO theory, which originally accounted only for the attractive van der Waals forces in a dielectric medium, is given by

$$V_H(r) = -\frac{A_H}{12}\left[\frac{\sigma_0^2}{r^2} + \frac{\sigma_0^2}{r^2 - \sigma_0^2} + 2\ln\frac{r^2 - \sigma_0^2}{r^2}\right] \tag{3}$$

where A_H is the Hamaker constant. The DLVO potential is just the sum of eqs 1 and 3 for distances greater than $\sigma = \sigma_0 + \delta$, that is, $V(r) = V_{DH}(r) + V_H(r)$, where δ is the so-called Stern layer accounting for the finite size of counterions. We used the value $\delta = 18$ Å in our calculations.

The protein solution we considered was recently studied in ref 30 by means of SANS, and it consists of an aqueous lysozyme solution in the presence of a D_2O citrate buffer at different pH values. (See Table 1.) Lysozyme is a globular protein whose shape can be depicted as a prolate ellipsoid of revolution. According to ref 30, we assume its volume V_p is equal to $4(\pi/3)aab$, with $a = 13.5$ Å and $b = 21.9$ Å. As protein diameter in eqs 1 and 3, we took a value that is an average of previously adopted values for lysozyme, that is, $\sigma \approx 37$ Å. The net charge on the protein surface appearing in eq 1 was determined in ref 30 according to the experimental titration curve, and its value depends on the pH according to Table 1. The Hamaker constant A_H reported in eq 3 was determined as

Table 1. DLVO Models and Related Parameters at Different Ionic Strengths/pH[a]

Q [e]	I_s [M]	pH
14	0.035	2.8
12	0.081	4.2
10	0.102	5.07
9.0	0.124	6.04

[a]Protein charge Q is expressed in electron units [e] and the ionic strength I_s is in units of molarity [M].

dx.doi.org/10.1021/jp212048j | J. Phys. Chem. B 2012, 116, 2114–2120

follows. First, we note that for lysozyme in water/NaCl solutions (one of the most studied lysozyme solutions) there is an evident correlation between the second virial coefficient B_2 and the critical temperature T_{cr}, that is, $B_2(T_{cr}) \approx -5.3B_2^{HS}$,[4,10] where $B_2^{HS} = (2/3)\pi\sigma^3$ is the second virial coefficient of hard spheres of diameter σ. Therefore, the knowledge of the critical temperature T_{cr} of the system can be exploited to find the value of the Hamaker constant A_H because B_2 can be expressed as

$$B_2(T) = B_2^{HS} + 2\pi \int_\sigma^\infty r^2\{1 - \exp[-\beta V(r)]\}\, dr \quad (4)$$

where $\beta = 1/k_BT$. From now on, we take the ambient temperature to be $T = 293.15$ K unless otherwise specified. Because we do not know the critical temperature of our system, we must resort to some estimate obtained from a lysozyme solution under similar solution conditions. In particular, we used the estimate by Taratuta et al.;[33] that is, $T = T_{cr} \approx 273.5$ K for a solution in a sodium phosphate buffer at pH = 6.0 because their pH is close to the system we considered at the highest ionic strength $I_s = 0.124$ M. (See Table 1.) However, the ionic strength in the work by Taratuta was very different ($I_s = 0.6$ M), and thus we performed two independent fits of the Hamaker constant A_H at $I_s = 0.124$ and 0.6 M by exploiting eq 4 to match $B_2 = -5.3B_2^{HS}$. Subsequently, the two DLVO potentials with different Hamaker constants were used in Gibbs ensemble MC simulations to verify that the critical temperature was almost unchanged.[39] Then, in this work, we used the Hamaker constant A_H estimated at $I_s = 0.124$ M; that is, $A_H = 26.43$ kJ/mol. Obviously, we were forced to use this procedure in the absence of experimental B_2 data under the same solution conditions. Very recently, we have shown that the choice to perform the fit at $I_s = 0.6$ M can yield different results.[39] The same value of the Hamaker constant is then used for all ionic strengths reported in Table 1 because the DLVO theory is expected to fit experimental B_2 data over a broad interval of ionic strengths.[25,26]

Once the value of the Hamaker constant becomes known, the effective protein−protein potential of interaction is unequivocally determined according to the DLVO theory. The theoretical scattered intensity can be calculated by using the equation

$$I(k) = N_p(\Delta\rho)^2V_p^2P(k)S(k) \quad (5)$$

where N_p is the number of protein molecules per unit volume in the solution, V_p is the volume of a single protein, and $\Delta\rho = (\rho_p - \rho_s)$ is the scattering contrast, that is, the difference between the electron density of protein molecules and that of the solvent. As a value for the coefficient multiplying $P(k)S(k)$, we used the reported experimental value $N_p(\Delta\rho)^2V_p^2 = 1.02$ cm^{-1}.[30] Here we are interested in the low-intermediate k range; therefore, we neglect the background that adds up to eq 5 as a constant term for all k wave vectors.[40] $P(k)$ is the form factor, that is, the scattering from a single protein molecule after orientational averaging over its surface. To calculate the form factor, we used the following expression[22]

$$P(k) \equiv \langle |F(k)|^2 \rangle = \int_0^1 dr \left| \frac{3(\sin u - u\cos u)}{u^3} \right|^2 \quad (6)$$

where $u = kb[(a/b)^2r^2 + (1 + r)^2]^{1/2}$ and eq 6 is evaluated numerically by using Romberg integration.[41]

Finally, $S(k)$ appearing in eq 3 represents the structure factor, which contains information about effective protein interactions, that is, $S(k) = 1$ for an ideal gas. The structure factor is calculated in NVT MC simulations of the DLVO potential at the different ionic strengths reported in Table 1. According to ref 30, we fix the density of the system to 100 g/L, which corresponds to a reduced number density $\rho\sigma^3 \approx 0.247$. MC computer simulations were perfomed by initially putting 1024 or 2048 particles at random positions inside a cubic box with cubic periodic boundary conditions. We used a cutoff on the DLVO potential at $r = 3.5\sigma$. The system was initially equilibrated in 10^5 to 10^6 cycles, where a cycle consisted in an attempt to displace a particle with an acceptance rate between 0.4 and 0.5. The structure factor was then calculated through MC computer simulations consisting of 5×10^5 cycles as the average of the autocorrelation function of the particle density in the wave-vector space[37]

$$S(\mathbf{k}) = \frac{1}{N}\langle \rho_{\mathbf{k}}\rho_{-\mathbf{k}} \rangle \quad (7)$$

where $\rho(\mathbf{k})$ is the spatial Fourier transform of the number density $\rho(\mathbf{r}) = \sum_{i=1}^N \delta(\mathbf{r} - \mathbf{r}_i)$.

We note that our procedure is not a trivial fit of the experimental scattered intensity reported in ref 30. The apparent success of a number of colloidal models, no matter how the attractive interactions between proteins are depicted, seems to indicate that the details of the adopted pair interaction potential are irrelevant, provided it is a short-range one. Within our model, the attractive interactions are modeled by means of the functional shape of the dispersion interaction. Therefore, our analysis will provide some insight into the validity of eq 1, that is, the linearized treatment of the Poisson−Boltzmann equation. The chosen pH values (see Table 1) are low enough to be in the regime of solution conditions where B_2 is monotonically decreasing as a function of the ionic strength,[25] and thus the DLVO model is expected to be still meaningful. Otherwise, a model with a discrete charge pattern on the protein surface[18,30] must be used or a model accounting for the inherent anisotropy of protein interactions.[42]

The structure factor was also calculated by means of the hypernetted-chain (HNC) and Percus−Yevick (PY) integral equations closures[37,38] to the Ornstein−Zernike equation

$$h(r) = c(r) + \rho \int c(|\mathbf{r} - \mathbf{r}'|)h(r')\, d\mathbf{r}' \quad (8)$$

where $h(r) = [g(r) - 1]$ and $c(r)$ are the pair and direct correlation functions, respectively, and $g(r)$ is the radial distribution function (rdf). The structural functions were calculated by using a Picard algorithm[38] on a grid extended up to 20.48σ, and the structure factor was obtained as

$$S(k) = \frac{1}{1 - \rho\tilde{c}(k)} \quad (9)$$

where $\tilde{c}(k)$ is the Fourier transform of the direct correlation function.

III. RESULTS AND DISCUSSION

In Figure 1, we plot the DLVO potentials at the ionic strengths/pH reported in Table 1. The case of lowest ionic strength is represented by the first potential from the top (see Figure 1), which is purely repulsive for all distances. The other potentials reported in Figure 1 exhibit a definite negative

dx.doi.org/10.1021/jp212048j | J. Phys. Chem. B 2012, 116, 2114−2120

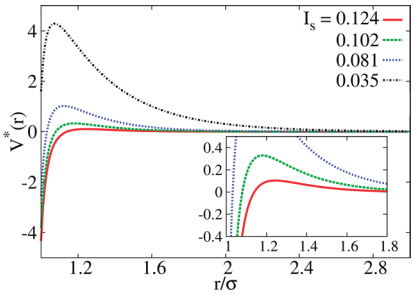

Figure 1. DLVO interaction potentials $V^*(r) = \beta V(r)$ as a function of the reduced distance for different ionic strengths.

minimum, which becomes deeper on increasing the solution ionic strength.

At the same time, we observe the progressive lowering of the potential maximum that shifts from $r^* = r/\sigma \approx 1.08$ at $I_s = 0.035$ to $r^* \approx 1.23$ at $I_s = 0.124$. We note that even if the maximum appears to be nearly negligible on the scale of Figure 1, it remains slightly different from zero (inset of Figure 1), displaying a long-range repulsive character. We will see later that this feature is able to generate a nontrivial physical effect. In general, the observed trend of the DLVO potentials is a consequence of the enhancing of the Debye constant (see eq 2) on increasing the ionic strength of the solution. Then, the DLVO potential becomes predominantly attractive and short-range at high ionic strengths. We note that the DLVO potentials at the higher pH develop an attractive depth at $\approx 4k_BT$, which is comparable to the one reported in refs 35 and 36, where a short-range attractive potential complemented by a Yukawa-screened electrostatic repulsion was adopted to describe the structural properties of salt-free lysozyme solutions. Under excess salt, the Yukawa energy contribution of refs 35 and 36 becomes identical to the repulsive part of the DLVO potential. It is worth noting since now that for these potential parameters, Cardinaux et al.[35,36] observe the formation of clusters resulting from the competition of the short-range attraction and the long-range repulsion.

Now, let us consider the rdf's at the lower ionic strengths/pH in Figures 2 and 3. At short distances, we clearly see the

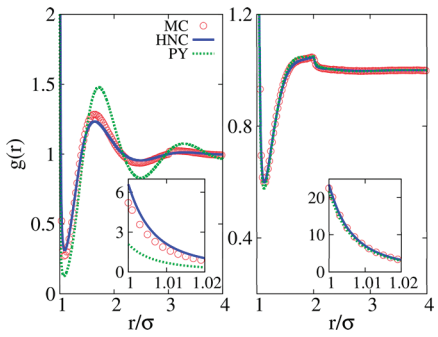

Figure 2. Radial distribution functions as a function of the distance at the ionic strength $I_s = 0.035$ M (left panel) and $I_s = 0.081$ M (right panel). Insets: plot enlargement near the distance of close contact between two particles. See the legend for the meaning of the lines/symbols.

presence of a depletion region for particles (first local minimum from the left), which becomes less important on increasing the ionic strength. At the same time, the minimum, which signals the presence of this region, shifts slightly to longer distances.

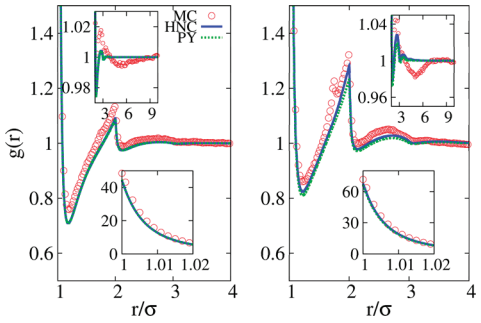

Figure 3. Radial distribution functions as a function of the distance at the ionic strength $I_s = 0.102$ M (left panel) and $I_s = 0.124$ M (right panel). Bottom insets: plot enlargement near the distance of close contact between two particles. Top insets: zoom out to show the behavior of the rdf at large distances. See caption of Figure (Figure 2) for the meaning of lines/symbols.

Both of the two features are explained in terms of the mechanism of repulsion-diminishing/attraction-enhancing when the Coulombic-screened part of the DLVO potential becomes significantly smaller than the Hamaker part. In fact, particles tend to stay closer to each other when the DLVO minimum is enhanced, making it more difficult for additional particles to find enough free volume to approach them. Then, the minimum of the depletion region moves to higher distances when the ionic strength increases and it becomes less pronounced. Obviously, the same mechanism explains the enhancement of the values of the rdf at contact (i.e., at a distance equal to one protein diameter) when the ionic strength increases. At the higher ionic strength (see right panel of Figure 3), the rdf shows the typical split of the second peak, which is characteristic of amorphous solids and glasses.[43]

An interesting aspect emerges when assessing the performance of the IETs in comparison with the MC data. The HNC appears slightly superior to the PY for any considered ionic strength and markedly superior for the lowest ionic strengths (see Figures 2 and 3). Whereas it is somewhat expected that the HNC theory performs better than the PY theory for long-range potentials,[38] the reverse should happen when the pair potential becomes more short-range. This evidence suggests that the DLVO potentials at the higher ionic strengths are more long-range than they appear on the expanded scale of eq 1. The long-range behavior of the MC rdf, reported in the upper inset of Figure 3, supports this conjecture. Apparently, the HNC and the PY closures are not able to capture the long-range correlations induced by DLVO potential at higher ionic strengths.

In Figures 4−7 we report the MC computer simulation and experimental intensities $I(k)$ (see eq 5) at different ionic strengths, along with the MC structure factor $S(k)$ (insets of Figures 4−7). The latter is also compared with $S(k)$ as obtained from HNC and PY theories. $S(k)$ for a fluid at liquid density usually exhibits peaks of decreasing height, which develop at some characteristic wave vectors. These peaks signal the length scales associated with the structuring of the fluid into coordination shells around a generic particle of the liquid. However, the system we considered has a low-intermediate density ($\rho\sigma^3 = 0.247$), very far from the liquid-state regime ($\rho\sigma^3 \approx 0.7$ to 0.9). Therefore, it is not surprising that the emerging shape for the structure factor at the lowest ionic strength is somewhat flat (inset of Figure 4), with a tendency of the curves to become more and more "structured" when the ionic strength

dx.doi.org/10.1021/jp212048j | J. Phys. Chem. B 2012, 116, 2114−2120

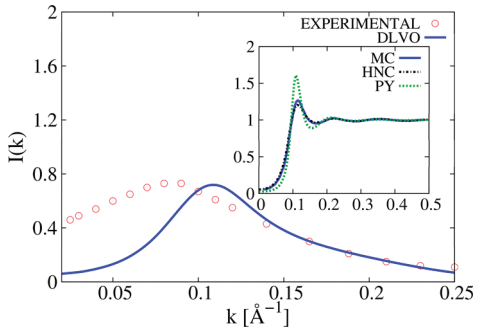

Figure 4. Main panel: experimental versus Monte Carlo computer simulation (DLVO) scattered intensity. Inset: structure factors according to Monte Carlo computer simulation and hypernetted chain (HNC) and Percus−Yevick (PY) integral equation theories.

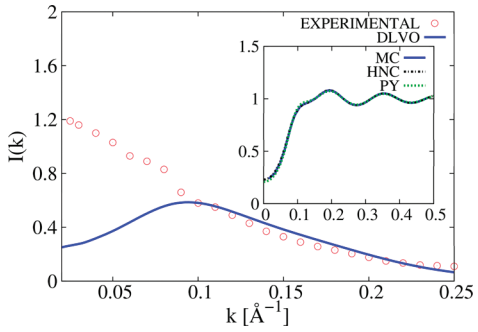

Figure 5. See the caption of Figure 4 for the meaning of lines/symbols.

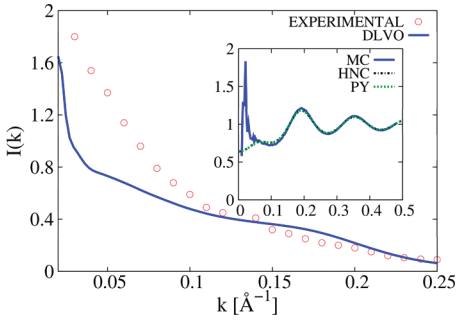

Figure 6. See the caption of Figure 4 for the meaning of lines/symbols.

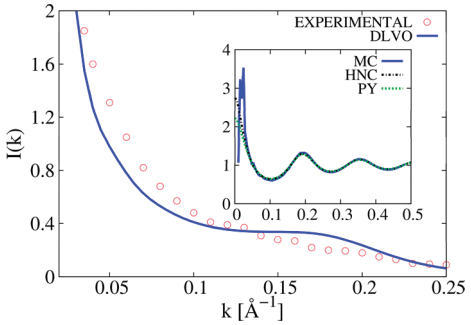

Figure 7. See the caption of Figure 4 for the meaning of lines/symbols.

increases (insets of Figures 5−7). The latter is again a consequence of the short-range attractive interaction, which enhances the local ordering among particles. The limit at zero wave vector of the structure factor is related to the value of the isothermal compressibility of the system.[37] By extrapolating the MC curves in the insets of Figures 4−7 to zero wave vector, we are then able to corroborate the expected result that the higher the ionic strength of the system the lower the compressibility of the system. The ability of colloidal potentials to account properly also for the decrease in the compressibility of the system when the volume fraction of protein is increased has also been observed recently.[36] We clearly see that the curve for the highest ionic strengths develops a sharp maximum at very low wave vector, which is not captured by the IETs (insets of Figures 6 and 7). Therefore, IETs seem unable to describe correlations among particles at long distance for higher ionic strengths, and we will comment about this drawback later. With the only exception of the lowest ionic strength (inset of Figure 4), where the HNC is markedly superior to the PY IET in reproducing the MC structure factor, both IETs are able to predict satisfactorily the short-range structure of the system (i.e., $S(k)$ at long k wave vectors).

At the lowest ionic strength I_s = 0.035 M, the experimental scattered intensity develops a maximum around $k_{max} \approx 0.09$ Å^{-1}, whose position is slightly overestimated by the theoretical calculation, that is, $k_{max} \approx 0.11$ Å^{-1} (Figure 4). This maximum is related to the existence of a well-pronounced peak of the structure factor at the same $k_{max} \approx 4k\sigma = 0.11$ Å^{-1}, as is apparent in the inset of Figure 4. This maximum is associated with the existence of correlations between particles at a distance approximately equal to two protein diameters, that is, $r \approx 60$ Å, and it also suggests the dominance of repulsive effects, which tend to correlate particles at large distances. This picture is qualitatively expressed by the DLVO model, which predicts that at this ionic strength protein interactions are purely repulsive because of the predominance of electrostatic effects, as is shown in Figure 4.

Increasing the ionic strength to I_s = 0.081 M (Figure 5) changes the character of the experimental scattered intensity, which now shows a monotonously decreasing trend as a function of the wave vector. This trend is evidently associated with the increase in density correlations at long distances (according to the definition of the structure factor $S(k)$, eq 7). If this increase were associated with a true divergence of the structure factor at k = 0, then the isothermal compressibility χ_T of the system ($\chi_T \propto S(0)$) would diverge, and this would in turn signal the proximity to the spinodal of a phase separation. However, because we do not have the experimental knowledge of $I(k)$ at very low wave vectors, we cannot draw this conclusion safely. Another possibility would be that protein aggregates with a characteristic length scale are forming in the system, and they determine the high values of $I(k)$ at low wave vectors. This picture is supported by the theoretical calculation, as we will see later. The MC computer simulation intensity fails to reproduce the correct trend even qualitatively because it continues to predict a maximum in the scattered intensity. However, for $k \geq 0.1$ Å^{-1}, the experimental intensity turns out to be reproduced quite reasonably. (See Figure 5.) Therefore, for this range of wave vectors the numerical structure factor reported in the inset of Figure 5 becomes reliable in reproducing the real correlations among particles of the system.

Increasing the ionic strength of the system further to I_s = 0.102 M makes the DLVO qualitatively correct in predicting the behavior of $I(k)$ at low wave vectors (Figure 6). The clear trend that emerges on increasing the ionic strength from I_s = 0.035 to 0.102 M is the progressive prevalence of attractive

dx.doi.org/10.1021/jp212048j | J. Phys. Chem. B 2012, 116, 2114−2120

interactions between proteins in comparison with repulsive interactions (Figure 1). Even if the DLVO theory fails to reproduce this trend quantitatively, it clearly appears that the DLVO $I(k)$ at low k systematically increases in going from I_s = 0.035 to 0.124 M. As shown in the inset of Figures 4–6, this behavior is driven by $S(k)$, illustrating that the DLVO model is able to describe qualitatively the enhancement of density correlations at low wave vectors (i.e., on large length scales), when increasing the ionic strength of the system.

The DLVO model is always quantitative in the intermediate-high range of wave vectors $k \geq 0.1$ Å^{-1}, as was pointed out before and as emerges by looking at Figures 4–6. If we observe the structure factor reported in the inset of Figure 6, then we note that the secondary peak develops around $6k\sigma - 7k\sigma \approx 0.2$ Å^{-1}, signaling the existence of protein correlations at a distance on the order of the protein diameter itself. This peak of the structure factor is then compatible with an aggregation of proteins, and this picture is also supported by the high values of the rdf close to contact, which is reported in the bottom insets of Figures 2 and 3. The high values of $I(k)$ are determined by the presence of a peak at the very small wave vector $k\sigma \approx 0.82$ or $k \approx 0.02$ Å^{-1}. (See the inset of Figure 6.) We will comment about its physical meaning later.

Finally, at the highest considered ionic strength I_s = 0.124 M, the experimental $I(k)$ is reproduced quantitatively by the DLVO theory, as shown in Figure 7. As it is apparent in Figure 1 (see bottom red line), in this limit, the DLVO potential exhibits the deepest attractive minimum, and the short-range attraction becomes overwhelmingly predominant in comparison with the long-range repulsion. It is interesting to note that in globular protein solutions protein crystals generally coexist with a fairly dilute protein solution, signaling the presence of short-range attractive interactions between proteins. This observation can explain the ability of the DLVO model to reproduce the experimental scattered intensity for high ionic strengths as well as its ability to describe the phase diagram. The partial inadequacy of the DLVO theory at low ionic strength is likely to be determined by the linearization of the Poisson–Boltzmann equation, which was assumed to obtain eq 1. Because according to eq 1 the Debye constant is associated with the exponential decay of the electrostatic repulsion as a function of the distance r, its inverse κ_D^{-1} represents an estimate of the length of the diffuse layer of counterions surrounding the protein. In fact, eq 1 is a reasonable approximation provided the screening layer is sufficiently compact, that is, $\kappa_D\sigma > 1$.

Similarly as for the case of ionic strength I_s = 0.102 M, we clearly see that the structure factor reported in the inset of Figure 7 develops a sharp maximum at a very low wave vector. The presence of these peaks can also be read in the upper insets of Figure 3, where the rdf's exhibit a slightly depleted region over a distance compatible with the wave vector of the peak. The plausible physical picture we can draw to justify the presence of these peaks at low wave vector is the existence of clusters/protein aggregates whose typical spacing is dictated by the maximum at $k\sigma \approx 0.82$ or $k \approx 0.02$ Å^{-1}, corresponding to a distance ≈ 300 Å, that is, ≈ 7 to 8 protein diameters. Whereas data related to the experimental intensity are not available for $k < 0.03$ Å^{-1}, the tendency of real protein solutions to form clusters has been reported in the literature,[32,35,36,44] and the theoretical prediction is supported by this evidence. Because of the nondynamical nature of the present study, we cannot make any certain conclusions related to the nature of these protein aggregates, that is, whether they are permanent clusters or the result of the formation of an intermediate-range order structure[23] that is determined by the shape of the pairwise potential. Further studies of the molecular dynamics of the present model would be useful to resolve this issue. At the same time, it is well-known that pair potentials, where there is competition between the short-range attraction and the long-range repulsion of the interaction energy, are able to generate different structural rearrangements, including clusters.[45] Recently, SANS and neutron spin echo (NSE) measurements[23] provided some evidence that the appearance of the low-k peak is not directly correlated to cluster formation because the lysozyme aggregates are found to have a finite lifetime. However, the presence of equilibrium clusters is strongly dependent on the experimental conditions. In fact, when the experiments are performed at ambient (high) temperatures, the balance in the competition between the short-range attraction and the Coulomb long-range repulsion is shifted toward the latter. Therefore, the monomers fail to condense at short distances and cluster formation is reduced. Similarly, at low pH values, lysozyme carries a higher net charge, which also enhances Coulomb repulsion, and cluster formation becomes unlikely, as we have also shown through our data. (See Figures 4 and 5.) On the contrary, the existence of long-lived equilibrium clusters becomes possible at low enough temperatures and high enough protein concentrations, as it has been unambiguously demonstrated in a recent paper by Cardinaux and coworkers[36] through a number of complementary tools, including SAXS, NSE, rheology, and computer simulations.

We note that for the mechanism of competition between the opposite forces in the colloidal potential to become effective it is necessary that the ratio of the attractive well depth to the repulsive potential barrier reaches a threshold value. This could explain why we do not also observe the same phenomenon for the ionic strength I_s = 0.081 M, which also exhibits a negative minimum (blue line of Figure 1). As is apparent in the insets of Figures 3 and 7, HNC and PY are not able to describe the highly inhomogeneous cluster/intermediate-range structure formation. A possible explanation might be that IETs hinge upon the assumption of homogeneous conditions.[37] However, it was recently shown[45] that enforcing a thermodynamic self-consistency criterion makes IETs able to predict the low-k peak of $S(k)$, which is frequently associated with cluster-like structuring of the system. This evidence is particularly promising with a view to applying more sophisticated IETS to describe accurately the structural functions of colloidal dispersions.

IV. CONCLUSIONS

We have applied the DLVO model to predict the structural behavior of lysozyme solutions under different conditions of pH/ionic strength. The DLVO theory is shown to be able to describe, in general, the tendency of protein interactions to become more short-range and attractive as the pH/ionic strength increases. This is determined by the progressive ion screening of the protein surfaces, which is described within the DLVO theory in terms of the enhancing of the Debye constant. However, this mechanism is reproduced only qualitatively for low ionic strenghts ($I_s \leq 0.102$ M), and the scattering intensity profile turns out to be correctly predicted by DLVO theory only for wavevectors $k \geq 0.1$ Å^{-1}, that is, for distances not greater than a couple of protein diameters.

The experimental scattered intensity becomes reasonably reproduced by the DLVO model throughout the whole range of wave vectors at sufficiently high ionic strength (I_s = 0.124 M). Under these solution conditions, DLVO theory indicates that protein aggregation takes place as a result of the competition between the short-range attractive and long-range repulsive energetic contributions of the pair interaction potential.

AUTHOR INFORMATION

Corresponding Author

*E-mail: pellicane@ukzn.ac.za.

Notes

The authors declare no competing financial interest.

ACKNOWLEDGMENTS

I acknowledge Prof. Carlo Caccamo for useful and enlightening discussions and Prof. Roger E. Raab for a careful reading of the manuscript. I also acknowledge the kind support of the College of AES, Dean of Research, Prof. Deogratius Jaganyi.

REFERENCES

(1) Jones, S.; Thornton, J. M. *Proc. Natl. Acad. Sci. U.S.A.* **1996**, *93*, 13−20.
(2) Klein, D. J.; Moore, P. B.; Steitz, T. A. *J. Mol. Biol.* **2004**, *340*, 141−177.
(3) Chayen, N. E. *Trends Biotechnol.* **2002**, *20*, 98.
(4) Muschol, M.; Rosenberger, F. *J. Chem. Phys.* **1997**, *107*, 1953.
(5) Tozzini, V. *Curr. Opin. Struct. Biol.* **2005**, *15*, 144−150.
(6) Louis, A. A.; Bolhuis, P.; Hansen, J. P.; Meijer, E. J. *Phys. Rev. Lett.* **2000**, *85*, 2522−2525.
(7) Frenkel, D. *Physica A* **2002**, *313*, 1−31.
(8) Muschol, M.; Rosenberger, F. *J. Chem. Phys.* **1995**, *103*, 10424.
(9) McPherson, A. *Preparation and Analysis of Protein Crystals*; Krieger: Malabar, FL, 1982.
(10) George, A.; Wilson, W. *Acta Crystallogr.* **1994**, *50*, 361−365.
(11) Rosenbaum, D. F.; Zamora, P. C.; Zukoski, C. F. *Phys. Rev. Lett.* **1996**, *76*, 150−153.
(12) Lomakin, A.; Asherie, N.; Benedek, G. B. *J. Chem. Phys.* **1996**, *104*, 1646.
(13) ten Wolde, P. R.; Frenkel, D. *Science* **1997**, *277*, 1975−1978.
(14) Hagen, M. H. J.; Frenkel, D. *J. Chem. Phys.* **1994**, *101*, 4093.
(15) Rosenbaum, D. F; Kulkarni, A.; Ramakrishnan, S.; Zukoski, C. F. *J. Chem. Phys.* **1999**, *111*, 9882.
(16) Haas, C.; Drenth, J.; Wilson, W. W. *J. Phys. Chem. B* **1999**, *103*, 2808−2811.
(17) Lomakin, A.; Asherie, N.; Benedek, G. B. *Proc. Natl. Acad. Sci. U.S.A.* **1999**, *96*, 9465−9468.
(18) Allahyarov, E.; Lowen, H.; Hansen, J. P.; Louis, A. A. *Phys. Rev. E* **2003**, *67*, 051404.
(19) Malfois, M.; Bonnete, E; Belloni, L.; Tardieu, A. *J. Chem. Phys.* **1996**, *105*, 3290.
(20) Tardieu, A.; Verge, A. L.; Malfois, M.; Bonnete, F.; Finet, S.; Ries-Kautt, M.; Belloni, L. *J. Cryst. Growth* **1999**, *196*, 193−203.
(21) Beretta, S.; Chirico, G.; Baldini, G. *J. Chem. Phys.* **2000**, *33*, 8663.
(22) Zhang, R; Skoda, M. W. A.; Jacobs, R. M. J.; Martin, R. A.; Martin, C. M.; Schreiber, F. *J. Phys. Chem. B* **2007**, *111*, 251−259.
(23) Liu, Y.; Porcar, L.; Chen, J.; Chen, W.-R.; Falus, P.; Faraone, A.; Fratini, E.; Hong, K.; Baglioni, P. *J. Phys. Chem. B* **2011**, *115*, 7238−7247.
(24) Piazza, R. *J. Cryst. Growth* **1999**, *196*, 415−123.
(25) Pellicane, G.; Costa, D.; Caccamo, C. *J. Phys. Chem. B* **2004**, *108*, 7538−7541.
(26) Pellicane, G.; Costa, D.; Caccamo, C. *J. Phys.: Condens. Matter* **2003**, *15*, 375−384.
(27) Dubin, S. B.; Clark, N. A.; Benedek, G. B. *J. Chem. Phys.* **1971**, *54*, 5158.
(28) Derjaguin, B. V.; Landau, L. D. *Acta Physicochim. URSS* **1941**, *14*, 633−652.
(29) Verwey, E. J. W.; Overbeek, J. T. G. *Theory of the Stability of Lyophobic Colloids*; Elsevier: Amsterdam, 1948.
(30) Abramo, M. C.; Caccamo, C.; Calvo, M.; Nibali, V. C.; Costa, D.; Pellicane, G.; Ruberto, R.; Toscano, R.; Wanderlingh, U. *Philos. Mag.* **2011**, *91*, 2066−2076.
(31) Frenkel, D.; Smit, B. *Understanding Molecular Simulation*; Academic Press: San Diego, 2001.
(32) Stradner, A.; Sedgwick, H.; Cardinaux, R; Poon, W. C. K.; Egelhaaf, S. U.; Schurtenberger, P. *Nature* **2004**, *432*, 492−195.
(33) Taratuta, V. G.; Holschbach, A.; Thurston, G. M.; Blankschtein, D.; Benedek, G. *J. Phys. Chem.* **1990**, *94*, 2140−2144.
(34) Pinsen, P.; Odijk, T. *J. Chem. Phys.* **2004**, *121*, 6525.
(35) Cardinaux, F; Stradner, A.; Schurtenberger, P.; Sciortino, F; Zaccarelli, E. *Europhys. Lett.* **2007**, *77*, 48004.
(36) Cardinaux, R; Zaccarelli, E.; Stradner, A.; Bucciarelli, S.; Farago, B.; Egelhaaf, S. U.; Sciortino, R; Schurtenberger, P. *J. Phys. Chem. B* **2011**, *115*, 7227−7237.
(37) Hansen, J. R.; McDonald, I. R. *Theory of Simple Liquids*; Academic Press: London, 1976.
(38) Caccamo, C. *Phys. Rep.* **1996**, *274*, 1−105.
(39) Abramo, M. C.; Caccamo, C; Costa, D.; Pellicane, G.; Ruberto, R.; Wanderlingh, U. *J. Chem. Phys.* **2012**, *136*, 035103.
(40) Chen, S. H. *Rev. Phys. Chem.* **1986**, *37*, 351−399.
(41) Press, W. H.; Flannery, B. P.; Teukolsky, S. A.; Vetterlin, W. T. *Numerical Recipes*; Cambridge University: New York, 1986.
(42) Pellicane, G.; Smith, G.; Sarkisov, L. *Phys. Rev. Lett.* **2008**, *101*, 248102.
(43) Tobochnik, J.; Chapin, P. M. *J. Chem. Phys.* **1988**, *88*, 5824.
(44) Lonetti, B.; Fratini, E.; Chen, S. H.; Baglioni, P. *Phys. Chem. Chem. Phys.* **2004**, *6*, 1388−1395.
(45) Kim, J. M.; Castaiieda-Priego, R.; Liu, Y.; Wagner, N. J. *J. Chem. Phys.* **2011**, *134*, 064904.